

## REVIEW OF ANTISKID AND BRAKE DYNAMICS RESEARCH

Sandy M. Stubbs and John A. Tanner  
NASA Langley Research Center

### SUMMARY

In an effort to establish the reasons for degraded performance of aircraft braking systems which sometimes occur on wet runways, Langley Research Center, with support from the FAA, has been involved in a program to study the behavior of various antiskid systems under the controlled conditions afforded by the Aircraft Landing Dynamics Facility. Results from this study utilizing a single main wheel of a DC-9 aircraft suggest that the systems investigated perform well under most circumstances but there may be room for improvement. For example, it has been demonstrated that pressure-bias-modulation can adversely affect the response of antiskid systems to rapid changes in the runway friction level. Results also indicate that antiskid systems designed to operate at a slip ratio of approximately 0.1 can provide a maximum braking effort without undue loss in the cornering capability of the tire. Time histories of braking friction coefficient were shown to provide a means of determining antiskid system performance and for systems that employed pressure-bias-modulation it was shown that performance could also be estimated from time histories of brake pressure and torque. Brake dynamic behavior from these tests has yielded the potential for more accurate mathematical models of the brake pressure-torque response which will be useful in future antiskid designs.

### INTRODUCTION

Over the years, the number and variety of airplanes using antiskid braking systems have steadily increased until now most current commercial and military jet airplanes are equipped with various skid control devices. The earliest antiskid systems were generally designed to prevent wheel lockups and excessive tire wear on dry pavements. Modern skid control devices, however, are more sophisticated and are designed to provide maximum braking effort while maintaining full antiskid protection under all weather conditions. Operating statistics of modern jet airplanes indicate that these antiskid systems are both effective and dependable; the several million landings that are made each year in routine fashion with no serious operating problems attest to this fact. However, it has also been well established, both from flight tests and from field experience, that the performance of these systems is subject to degradation on slippery runways; consequently, dangerously long roll-out distances and reduced steering capability can result during some airplane landing operations (refs. 1 to 3). Thus, there exists a need to study different types of antiskid braking systems in order to find reasons for the degraded braking performance that occurs under adverse runway conditions; there is also a need to obtain data for the development of more advanced systems that will insure safe ground handling operations under all weather conditions.

In an effort to meet these needs, an experimental research program was undertaken by NASA with support from the Federal Aviation Administration to study the single-wheel behavior of several different airplane antiskid braking systems under the controlled conditions afforded by the Langley Aircraft Landing Loads and Traction Facility. The types of skid control devices studied in this program included a velocity-rate-controlled system, a slip-ratio-controlled system with ground reference from an unbraked nose wheel, a slip-velocity-controlled system, and a mechanical-hydraulic system. The investigation of all these systems was conducted with a single main wheel, brake, and tire assembly of a McDonnell Douglas DC-9 series 10 airplane.

The purpose of this paper is to present some of the significant findings which became evident during the test of the antiskid systems under maximum braking effort. The parameters varied in the study included test speed, tire loading, tire yaw angle, tire tread condition, brake-system operating pressure, and runway wetness condition; a detailed discussion of the effects of these parameters on three of the systems studied can be found in references 4, 5, and 6. This paper touches briefly on several aspects of antiskid system design philosophy, discusses techniques for evaluating antiskid performance, and discusses brake dynamics during antiskid cycling.

## APPARATUS AND TEST PROCEDURE

### Test Facility

The investigation was performed using the test carriage shown in figure 1. Also shown in figure 1 is a close-up view of the test wheel and the instrumented dynamometer which was used instead of a landing-gear strut to support the DC-9 tire, wheel, and brake assembly because it provided an accurate measurement of the tire-ground forces. The test tire was a 40x14, type VII retreaded tire inflated to .97 MPa.

The test runway can also be seen in figure 1. Approximately 244 m of the flat concrete test runway were used to provide braking and cornering data on a dry surface, on an artificially damp surface, on an artificially flooded surface, and on a natural-rain wet surface. The test speeds used in the investigation were 50, 75, and 100 knots, and fixed tire yaw angles of 0, 1, 3, 6, and 9 degrees were examined. Vertical load was varied from 58 kN to 124 kN, and effects of three brake system pressures of 10, 14, and 21 MPa were studied.

### Skid Control Systems

The brake system hardware used in the investigation is shown in figure 2. The brake system components were a pilot metering valve, brake selector valve, and a hydraulic fuse, all DC-9 aircraft components. The antiskid control valve is peculiar to each antiskid system investigated. The line sizes and lengths were those of the DC-9 but line bends were not simulated.

A schematic of a typical brake system is shown in figure 3. The supply pressure is fed through the pilot metering valve (which for these tests was set to give maximum braking effort) to the antiskid control valve and on to the brake. A speed sensor located on the braked wheel was used as input to the antiskid control box (the heart of the system) which produces a signal to regulate the antiskid control valve.

Four antiskid systems have been tested in this investigation. A velocity-rate controlled and a slip-velocity controlled system both having pressure bias modulation as a key element in their logic circuits are similar to the schematic shown in figure 3. A slip-ratio controlled antiskid system was investigated that used (in addition to the items illustrated in the sketch of figure 3) an input from an unbraked nose wheel to obtain the aircraft ground speed. The fourth system tested was a mechanical-hydraulic system not at all like the schematic of figure 3; instead, it had an internal flywheel spun-up by the free rolling wheel through an over-running clutch before application of brakes. The speed of the flywheel was mechanically compared with the braked wheel speed so that when the braked wheel angular velocity decreased at a rapid rate, brake pressure was released.

## RESULTS AND DISCUSSION

The paragraphs in this section will discuss some factors that adversely affect antiskid performance on slippery runways; the use of pressure, torque, and friction information to estimate antiskid performance, and brake dynamics during antiskid cycling including the mathematical modeling of the brake pressure-torque response.

### Optimum Slip Ratio For Antiskid Control

The drag force friction coefficient is plotted as a function of slip ratio in figure 4 to illustrate the advantages of using slip ratio as the parameter for antiskid control. By definition, a slip ratio of one is a locked wheel skid, and a slip ratio of zero is a freely rolling tire. Figure 4 presents data for three separate runs at 0° yaw conditions on dry, damp, and flooded runway surfaces. During the course of antiskid cycling, hysteresis loops or eddies can be seen which result in variations in the drag force for a given slip ratio. The maximum drag force friction coefficient is shown to occur initially at about a 0.1 slip ratio and to hold fairly constant out to a slip ratio of approximately 0.4 for all three surface conditions.

The variation of the drag force friction coefficient and the corresponding side force friction coefficient with slip ratio is presented in figure 5 for a yawed tire undergoing braking on a damp concrete surface. Again, the maximum drag force friction coefficient occurs initially at about 0.1 slip ratio, as was shown in figure 4, but the maximum side force friction coefficient is shown to occur at 0 slip ratio when the tire is unbraked. Further-

more, the side force friction decreases rapidly such that at slip ratios above approximately 0.2 the tire cornering capability has been reduced to essentially an insignificant value. For this reason, a slip ratio of approximately 0.1 is suggested as the optimum for antiskid system design, since that value provides near-maximum braking force while retaining a fairly high percentage of the side force which is necessary for steering control.

If an antiskid braking system is to operate on the principle of slip ratio control, then measurements of the aircraft ground speed and the braked wheel speed are needed as inputs to the antiskid system logic circuits. Figure 6 shows braked wheel speed as a function of time for two different antiskid systems. The top curve is for a slip-ratio controlled antiskid system and the lower one is for a system without slip ratio control. The dashed lines on both plots indicate the ground speed decay of the aircraft, or in this case, the test carriage. The lower plot indicates that the system without slip ratio control cycled as designed with several instances wherein the brakes were released to permit the tire to spin up to the speed of the test carriage. Hence, for this system, the information from the braked wheel can be used to establish both the vehicle ground speed and the braked wheel speed.

On the other hand, the slip-ratio controlled system (top plot of figure 6) attempts to maintain the braked wheel speed at about 10% below the carriage ground speed for this test and, as such, never allows spin-up of the braked wheel to approach the carriage ground speed. Thus, for this type of system to properly function it is necessary to obtain a ground speed reference from some source independent of the braked wheel such as the unbraked nose wheel or an inertia platform.

### Antiskid System Control Logic

Figure 7 addresses the issue of pressure bias modulation and its effect on antiskid control. Pressure bias modulation is an antiskid logic design feature used on some systems to enhance performance by increasing the operating time on the front side (positive slope) of the  $\mu$ -slip curve. This logic may be satisfactory under conditions of constant available friction, but, as shown in figure 7, may be less satisfactory when friction surface conditions are changing rapidly. Time histories of wheel speed, skid signal, brake pressure, and drag force friction are presented in the figure for a test on a dry runway that has one damp spot about .6 m in diameter approximately midway down the test section. The figure shows that the wheel speed is cycling as designed on the dry surface such that wheel spin-down as at A causes a skid signal build-up B which closes the antiskid control valve, thereby reducing the brake pressure C. When the wheel spins back up D, the skid signal reduces and the brake pressure is reapplied. At approximately 6 seconds into the test, the wheel encounters the damp spot on the runway and immediately goes into a deep skid causing a saturated skid signal E and a corresponding reduction in brake pressure. When the wheel spins back up on this occasion the skid signal is only slightly reduced F because the pressure bias modulation system causes a slow reduction in skid signal and a consequent slow reapplication of



brake pressure G. The resulting drag force friction coefficient trace shows that while the tire is being braked on a dry surface, the friction coefficient is effectively maintained at a level of about .6, but when it reaches the damp spot, the friction coefficient drops abruptly and remains below that level over a considerable time period because of the slow rate of brake application following the deep skid. An ideal system would allow a rapid reapplication of the brake pressure and bring the friction coefficient back up quickly to take advantage of that available on the dry surface.

Figure 8 shows the same type of test but without pressure bias modulation in the antiskid system. Again, when the tire reaches the damp spot on the runway, the wheel speed drops suddenly, causing the skid signal to saturate with a corresponding drop in brake pressure. When the wheel spins back up, the skid signal drops almost immediately to zero since it is not modulated and the brake pressure is rapidly reapplied. The drag-force friction coefficient indicates good antiskid action since it drops only momentarily when the damp spot is encountered. This type of reaction should greatly enhance antiskid performance under variable runway friction conditions.

### Estimating Antiskid Braking Performance

References 7, 8, and 9 discuss several different sources from which antiskid-system efficiencies can be calculated. Ideally, antiskid efficiency should be based upon the friction developed between the tire and the runway surface. However, friction measurements are not readily obtained in practice and other characteristics such as brake torque or brake pressure must be employed. Figures 9, 10, and 11 are presented to illustrate the agreement, or lack thereof, between efficiencies as determined from friction, brake torque, and brake pressure measurements. Shown in figure 9 are typical time histories of brake pressure, torque, and friction for an antiskid system which employs pressure bias modulation. Following brake application, denoted by the rapid rise in all three measurements, the friction and brake torque gradually increase to maximum levels while the pressure is held constant, and when the tire enters into a deep skid all three drop suddenly. Four such cycles are observed during the course of the run shown. To compute the braking performance index (antiskid efficiency)  $\beta$ , the average pressure, torque, and friction developed during a run are divided by the respective average maximum value which, for this run, is the average of four measurements. Observe that for this test all three sources yielded essentially the same performance index.

Not all runs are as easy to analyze as the run shown in figure 9, however. Figure 10 presents time histories of the brake pressure, torque, and friction for a run on a wet surface using the same antiskid system. Maximum values for the pressure trace can be readily identified and when divided into the average value define a performance index of .81. The brake torque can also be analyzed in this fashion and gives an index of .80. The drag-force friction trace, however, shows no incipient skid points like those of the other two traces or like those in figure 9. In an effort to be unbiased, the maximum friction for such cases was taken at fixed time steps over the entire run. In

the run described by figure 10, when the average friction is divided by the maximum obtained by this technique, the performance index is computed to be .84. Thus, it appears that either pressure, torque, or friction may be used to obtain the performance index for this type of antiskid system.

Use of pressure or torque for determining antiskid performance can be misleading for a fast-responding antiskid system, however. Figure 11 shows time histories of brake pressure, torque, and friction for a slip-ratio controlled antiskid system that has high-frequency, high-amplitude oscillations in the brake pressure and torque traces. For this run, if the average pressure is divided by the maximum pressure, the resulting performance index is .77 and the index as computed from the brake torque is .85. In the friction trace, if the maximum friction values are obtained at fixed time intervals, a performance index of .91 is obtained. Thus, for this type of antiskid system, pressure and torque data will give estimates of braking performance which appear to be too low and the performance estimates based upon friction data should be used.

### Brake Dynamic Pressure-Torque Relationship

A major finding of this study of antiskid braking systems has been the discovery of the true nature of brake dynamic behavior while under antiskid control. The plots on the left side of figure 12 show typical examples of the pressure input to the brake during antiskid operation, the resulting torque output from the brake, and the relationship between the brake pressure and brake torque as observed during a typical antiskid-braking test. This pressure-torque relationship defines brake behavior during antiskid operations and plays a critical role in establishing the braking efficiency of an antiskid braking system. The relationship depicted in figure 12 is characterized by fairly large hysteresis loops which imply a wide range of torque values for a given pressure.

Computer simulations of antiskid braking systems are needed to tune existing antiskid systems to optimize their braking and cornering performance for specific aircraft applications and to aid in future antiskid system designs. Sometimes these simulations are used to estimate antiskid-system efficiencies. These computer simulations typically model the brake pressure-torque response either as a linear spring with viscous damping or as an undamped nonlinear spring. When these current models are exercised with the actual pressure input from a typical antiskid braking test, however, they do not adequately represent the complicated hysteresis conditions that routinely exist in the brake pressure-torque response, as shown on the right in figure 12.

Recently, a nonlinear hysteresis model was developed at the Langley Research Center that captures the essence of the brake response characteristic. This improved model is based upon a variable, nonlinear spring with coulomb or friction damping. When this model is exercised with the actual brake pressure input there is a significant improvement in the fidelity of the pressure-torque response. By comparing the torque outputs from each model with the actual torque response of the brake for the same pressure input it is possible

to carry out an error analysis, and the results of such an analysis based on percent torque error for each of the models are presented in the bar chart in the middle of the figure. The data indicate that the Langley model reduces the torque errors significantly. Currently this improved mathematical model is being introduced into a ground handling simulator to better represent antiskid control for future studies.

#### CONCLUDING REMARKS

The results obtained to date from a study of the single-wheel behavior of antiskid braking systems suggest that the systems investigated perform well under most circumstances but that there is room for improvement. For example, it was demonstrated that pressure-bias-modulation can adversely affect the response of aircraft antiskid braking systems to rapid changes in the runway friction level. The results of this study also indicate that antiskid braking systems designed to operate at a fixed slip ratio of approximately 0.1 can provide a maximum braking effort without undue loss in the cornering capability of the tire.

It was demonstrated that the braking performance of systems which employ pressure-bias-modulation can be estimated from time histories of the brake pressure or torque when friction data are not available.

Finally, data from these tests have provided significant insights into brake dynamic behavior during antiskid cycling and yield the potential for more accurate mathematical models of the brake pressure-torque response which will be useful in the design of future aircraft antiskid braking systems.

## REFERENCES

1. Tracy, William V., Jr.: Wet Runway Aircraft Control Project (F-4 Rain Tire Project). ASD-TR-74-37, U.S. Air Force, Oct. 1974. (Available from DTIC as AD A004 768).
2. Danhof, Richard H.; and Gentry, Jerauld R.: RF-4C Wet Runway Performance Evaluation. FTC-TR-66-6, U.S. Air Force, May 1966. (Available from DTIC as AD 486 049).
3. Horne, Walter B.; McCarty, John L.; and Tanner, John A.: Some Effects of Adverse Weather Conditions on Performance of Airplane Antiskid Braking Systems. NASA TN D-8202, 1976.
4. Stubbs, Sandy M.; and Tanner, John A.: Behavior of Aircraft Antiskid Braking Systems on Dry and Wet Runway Surfaces - A Velocity-Rate-Controlled, Pressure-Bias-Modulated System. NASA TN D-8332, 1976.
5. Tanner, John A.; and Stubbs, Sandy M.: Behavior of Aircraft Antiskid Braking Systems on Dry and Wet Runway Surfaces - A Slip-Ratio-Controlled System With Ground Speed Reference From Unbraked Nose Wheel. NASA TN D-8455, 1977.
6. Stubbs, Sandy M.; and Tanner, John A.: Behavior of Aircraft Antiskid Braking Systems on Dry and Wet Runway Surfaces - A Slip-Velocity-Controlled, Pressure-Bias-Modulated System. NASA TN D-1051, 1979.
7. Skid Control Performance Evaluation. ARP 862, Soc. Automot. Eng., Mar. 1, 1968.
8. Lester, W. G. S.: Some Factors Influencing the Performance of Aircraft Anti-Skid Systems. Tech. Memo. EP 550, British R.A.E., July 1973.
9. Brake Control Systems, Antiskid, Aircraft Wheels, General Specifications for Mil. Specif. MIL-B-8075D, Feb. 24, 1971.



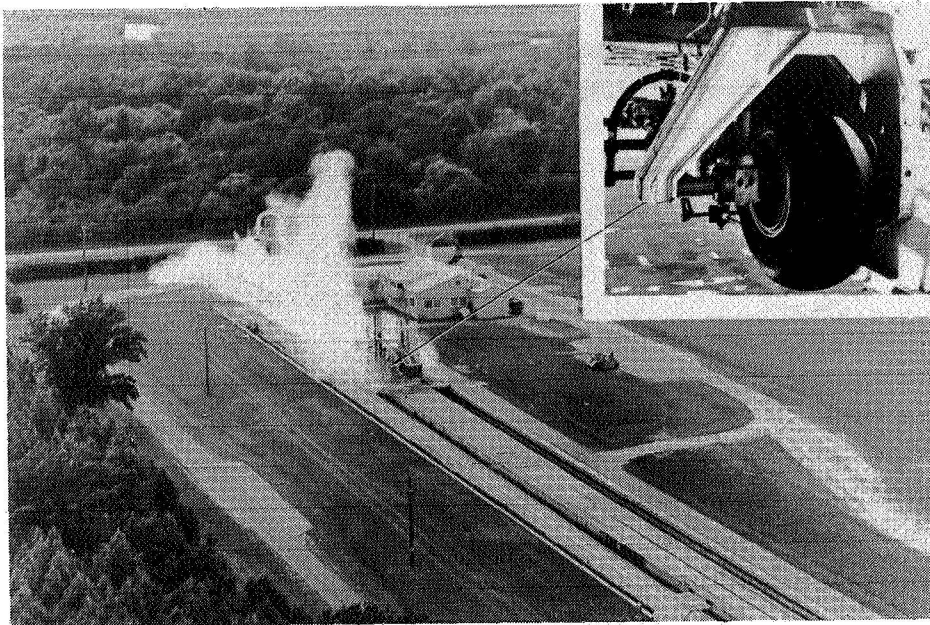


Figure 1.- Landing loads track test carriage.

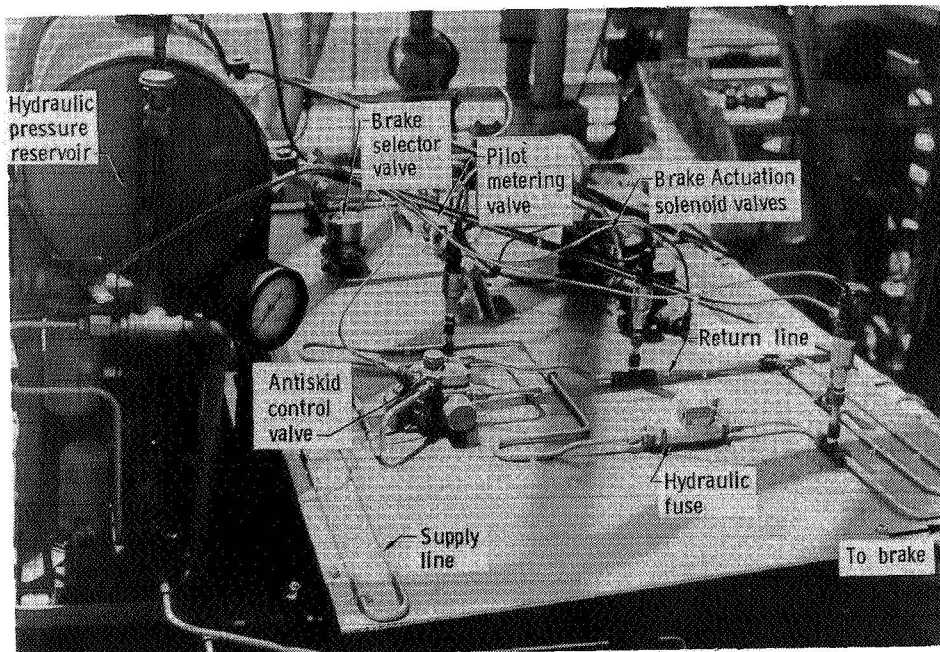


Figure 2.- DC-9 (Series 10) brake system simulation.



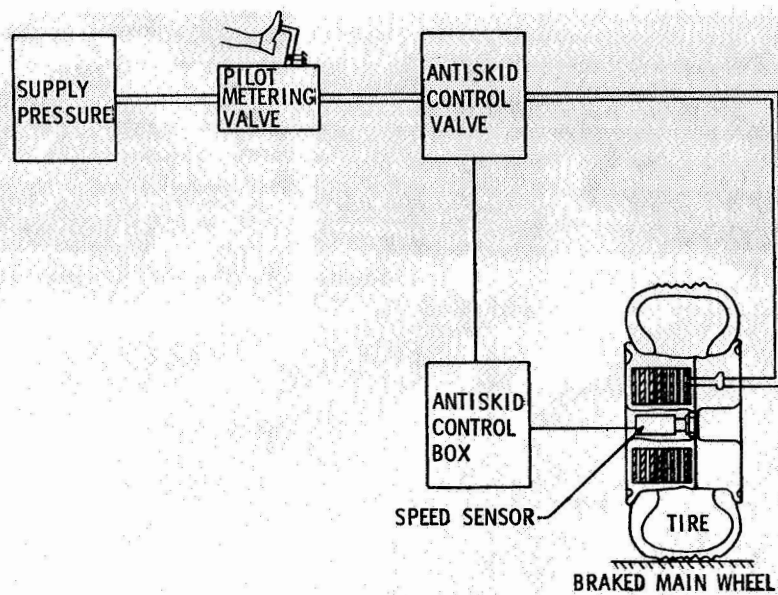


Figure 3.- Schematic of typical brake system.

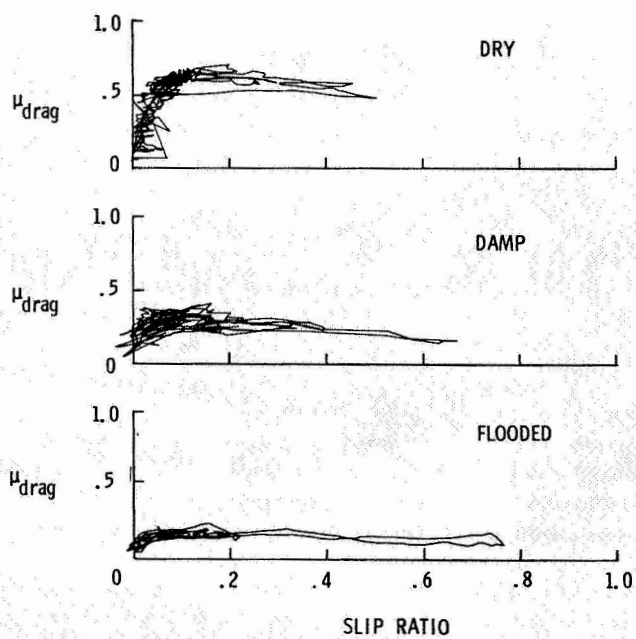


Figure 4.- Tire friction variations with slip ratio.

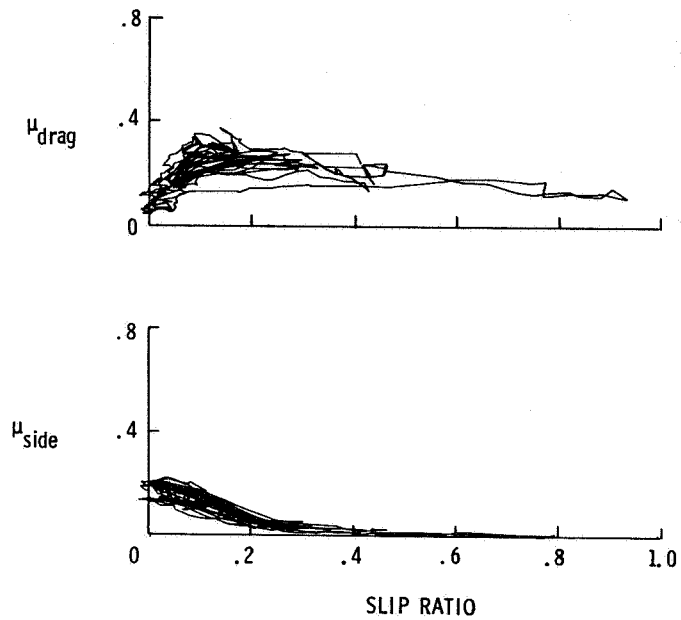


Figure 5.- Drag and side friction variations with slip ratio.

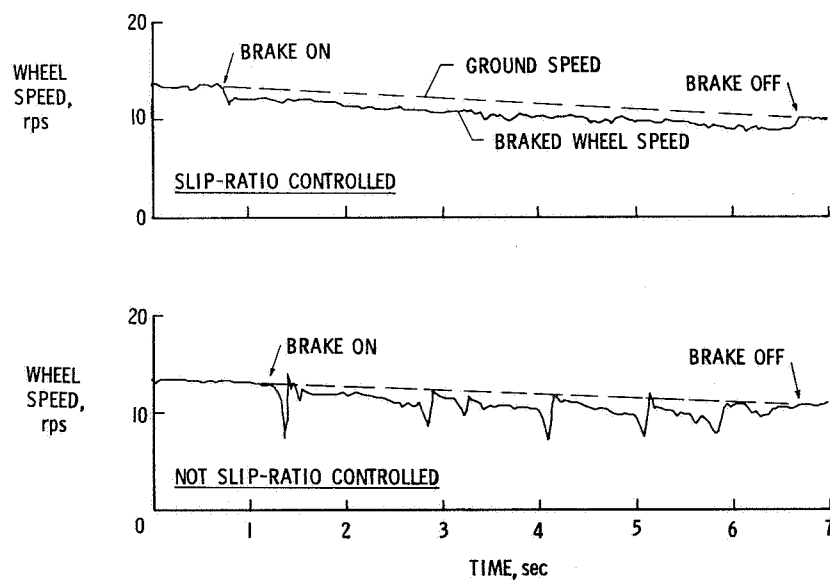


Figure 6.- Wheel speed response with and without slip-ratio control.

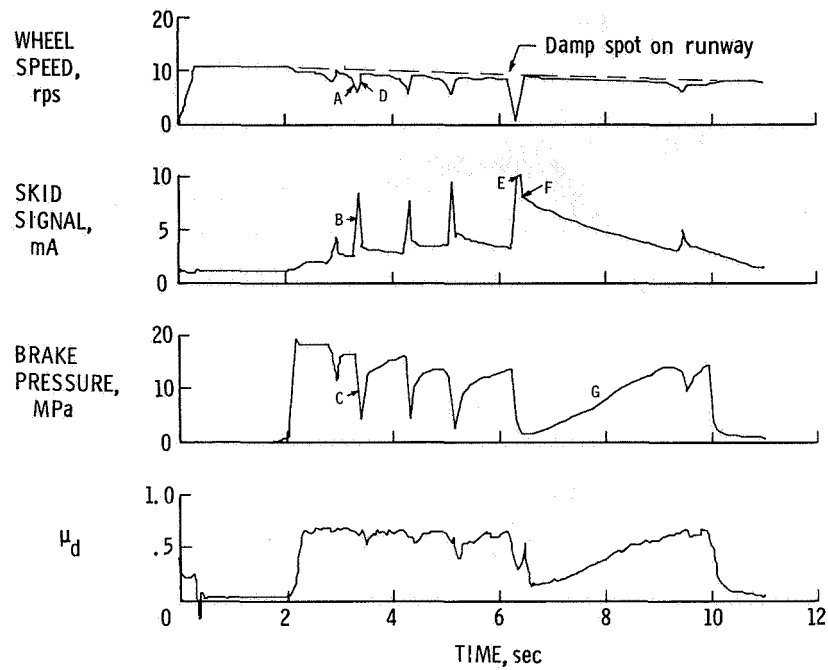


Figure 7.- Antiskid response with pressure bias modulation.

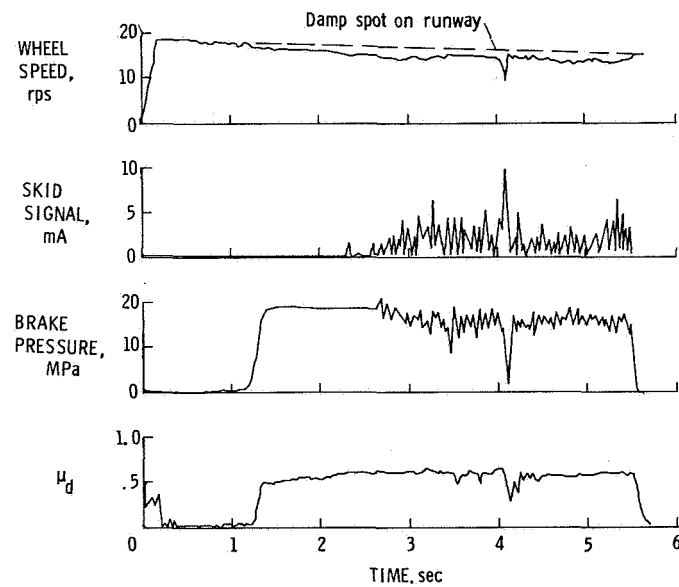


Figure 8.- Antiskid response without pressure bias modulation.

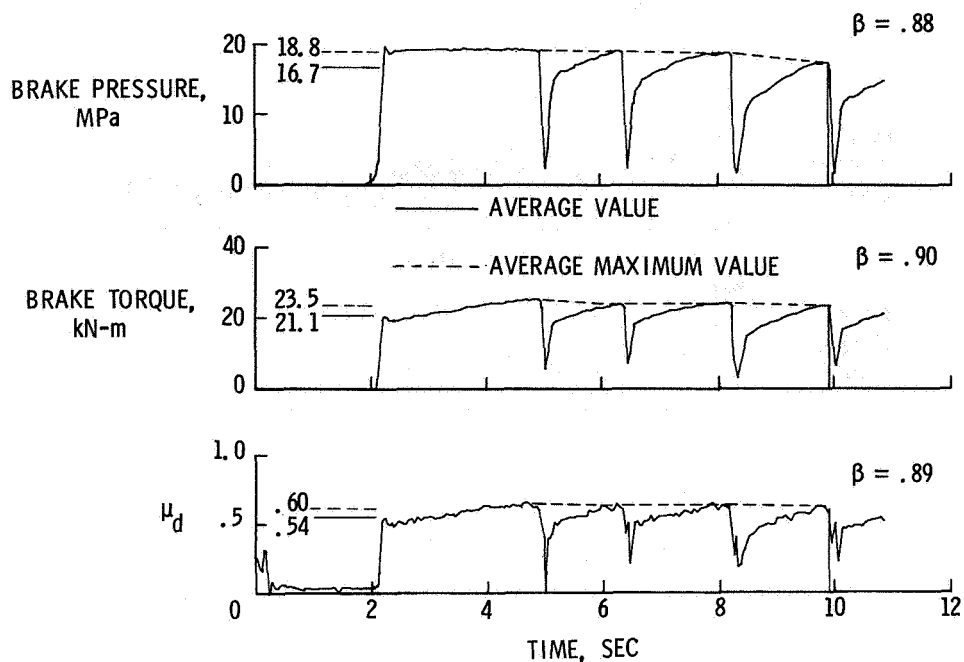


Figure 9.- Methods of estimating antiskid braking efficiency.  
 Antiskid with pressure bias modulation on a dry runway.

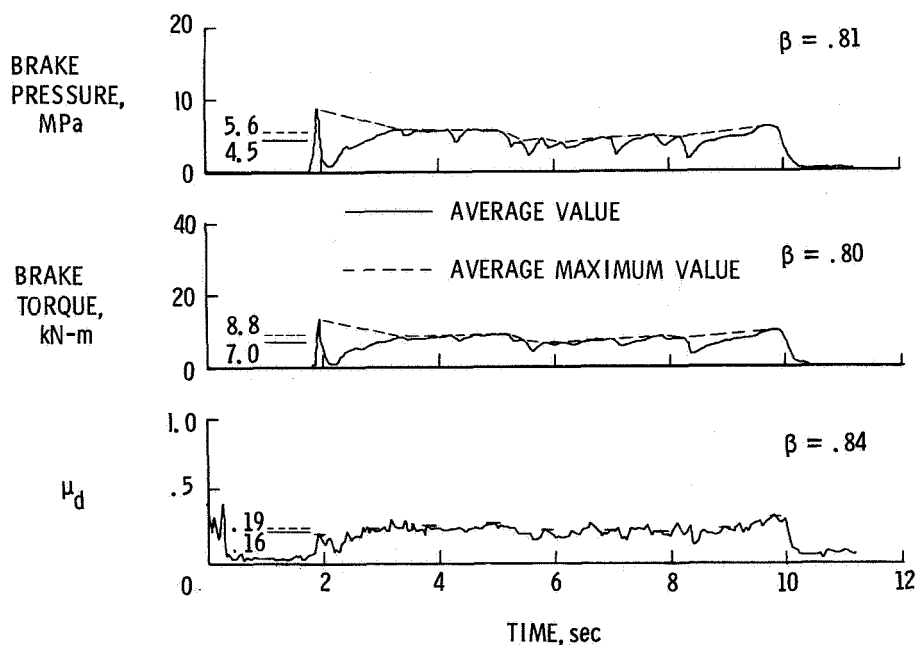


Figure 10.- Methods of estimating antiskid braking efficiency.  
 Antiskid with pressure bias modulation on a damp runway.



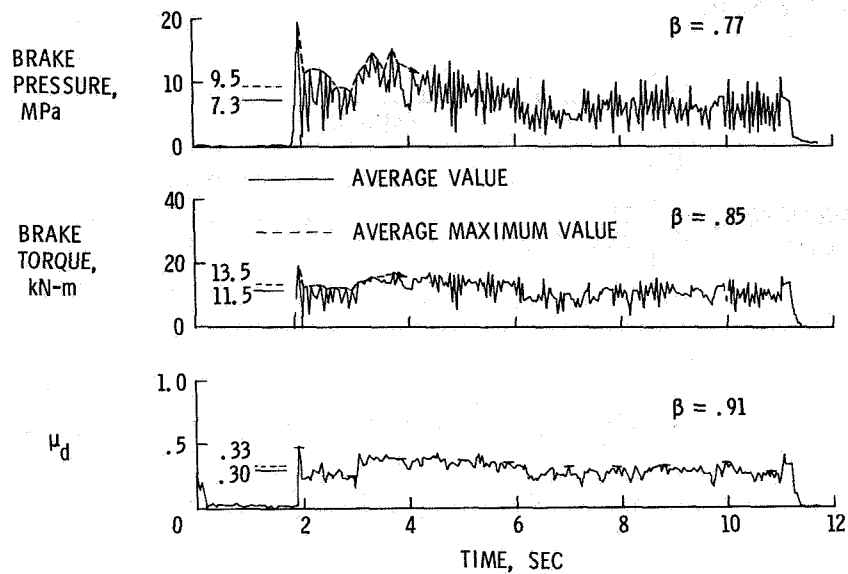


Figure 11.- Methods of estimating antiskid braking efficiency.  
 Antiskid without pressure bias modulation on a damp runway.

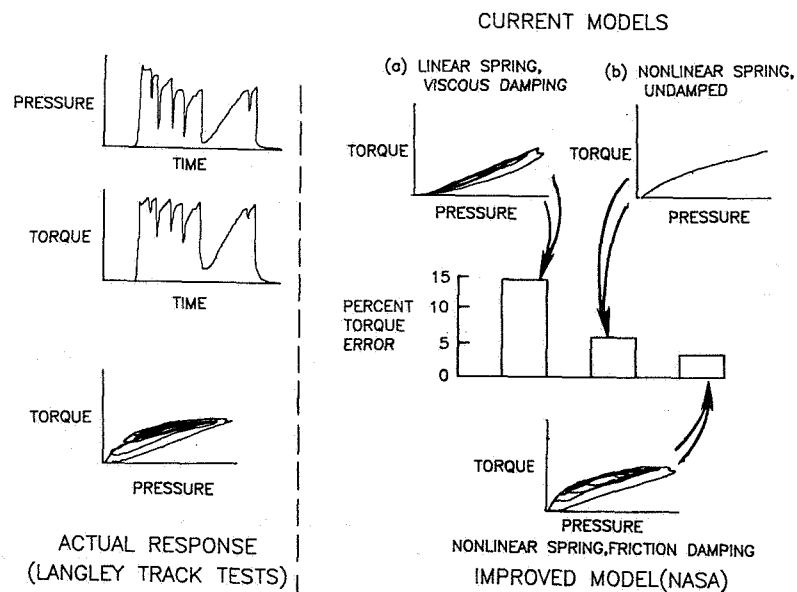


Figure 12.- Aircraft brake pressure-torque response.